On Atmospheric Energy Conversions Between the Zonal Flow and the Eddies

By A. WIIN-NIELSEN, JOHN A. BROWN and MARGARET DRAKE, *National Center for Atmospheric Research, Boulder, Colorado*

(Manuscript received May 27, 1963)

ABSTRACT

Energy transformations between the zonal mean and the eddies have been computed from observed data for a single winter month, January 1962. The available data were the height fields of the 850, 700, 500, 300 and 200 mb surfaces. Our calculations are therefore based on the geostrophic or balanced approximations. The horizontal fields of the streamfunction and the thickness are written as one-dimensional Fourier series, and the energy transformation between the zonal mean and the different longitudinal wave-numbers are evaluated. In order to evaluate the energy transformations in the wave number regime, it is necessary to compute the meridional transports of momentum and heat as a function of the wave number. These results appear therefore as useful by-products of the calculations.

The main conclusions which can be made on the basis of the calculations are:

1. The maximum transport of sensible heat occurs in the middle latitudes and at the lower elevations. More than 50% of the transport of sensible heat is carried out by wave numbers 1 to 4, while the next four wave numbers (5 to 8) transport half this amount.

2. The transport of momentum is toward the north south of about 55° N and toward the south north of this latitude. The maximum northward transport of momentum occurs at 35° N at higher elevations, while the maximum southward transport takes place at 65° N also at higher elevations. About 50% of the northward transport of momentum is carried out by wave numbers 1 to 4 and about 30% by the next four wave numbers (5 to 8).

3. The conversion of zonal available potential energy to eddy available potential energy is found to be positive for almost all wave numbers with a single maximum around the wave numbers 2 and 3.

4. The conversion of eddy kinetic energy to zonal kinetic energy is found to be positive when summed over all wave numbers. The conversion is much smaller than the conversion mentioned in 3. The spectrum is very irregular showing positive conversions for the small wave numbers, but negative conversions for some of the larger wave numbers.

The conclusions mentioned above are tentative, since they are based on data from a single winter month. Computations for other winter months and for other seasons are being planned.

1. Introduction

The equations for studies of the energetics of the atmosphere in the wave number regime were first treated systematically by SALTZMAN (1957). Since then it has been possible to compute some of the energy transformations from observed data. The transformation between eddy available potential energy and eddy kinetic energy has for example been computed by WIIN-NIELSEN (1959) and SALTZMAN and FLEISHER (1960*b*, 1961). The conversion of eddy kinetic energy to zonal kinetic energy in the domain of wave numbers was computed from 500 mb data alone by SALTZMAN and FLEISHER (1960*a*), whilst WIIN-NIELSEN and BROWN (1960) computed the generation of zonal and eddy available potential energy with the latter quantity expressed in the wave number space. In order to study the maintenance of the vertically integrated flow, it has furthermore been found advantageous to compute the energy conversion between the vertical mean flow and the deviation from this flow, the so-called vertical shear flow (WIIN-NIELSEN, 1962).

The calculations mentioned above do not give a complete picture of the energetics of the large-scale flow in the atmosphere for the following reasons. Some energy conversions, as for example the conversion of zonal available potential energy to eddy available potential energy, have not been computed in the domain of wave number according to the knowledge of the authors. The energy conversions which have been treated were in all cases computed with a very low vertical resolution, i.e. with only one or two information levels in each vertical column of the atmosphere. The energy conversions between available potential energy and kinetic energy, which requires a knowledge of the vertical velocity in the atmosphere, were computed under the assumption that the atmosphere is frictionless and adiabatic. While this assumption may be a good approximation for the higher wave numbers, it probably does not hold for the largest scales (i.e. the low wave numbers).

It is therefore needed to extend the calculations to the quantities not treated previously, to obtain a higher vertical resolution and to remove some of the assumptions if possible. In this paper we are going to describe the results of calculations of energy transformations between zonal and eddy available potential energy and between zonal and eddy kinetic energy in the wave number space. Since these calculations depend on the meridional transport of heat and momentum as functions of the wave number, we will obtain these quantities as important by-products.

2. Conversion between zonal and eddy available potential energy

Due to the nature of the available data which consist of height data only, it is necessary to apply the quasi-geostrophic or balanced theory. We shall therefore begin by considering the expressions for the different energy conversions as they appear in this theory. The thermodynamic equation will first be considered in order to obtain an expression for the rate of change of available potential energy. It is sufficient to consider the rate of change of zonal available potential energy. The most convenient form of the thermodynamic equation for use in the quasi-geostrophic theory is

$$\frac{\partial}{\partial t}\left(\frac{\partial \Phi}{\partial p}\right) + \mathbf{V}\cdot\nabla\left(\frac{\partial \Phi}{\partial p}\right) + \sigma\omega = -\frac{R}{c_p}\frac{1}{p}\frac{dQ}{dt}, \quad (2.1)$$

in which $\Phi = gz$ is the geopotential, g the acceleration of gravity, z the height of an isobaric surface, $\mathbf{V}$ the horizontal velocity vector with components u (eastward) and v (northward), $\omega = dp/dt$ the vertical "velocity".

$$\sigma = -\frac{\alpha}{\theta}\frac{\partial \theta}{\partial p}$$

a measure of static stability, α the specific volume, θ the potential temperature, p pressure, R the gas constant, c_p specific heat for constant pressure and dQ/dt the amount of heat added to the atmosphere per unit mass and unit time. In the balanced theory $\mathbf{V}$ is considered to be non-divergent, but the form of the continuity equation is still

$$\nabla\cdot\mathbf{V} + \frac{\partial \omega}{\partial p} = 0. \quad (2.2)$$

Furthermore $\sigma = \sigma(p)$, is a function of pressure only in the balanced theory. For convenience in the later calculations we express (2.1) and (2.2) in spherical coordinates

$$\frac{\partial}{\partial t}\left(\frac{\partial \Phi}{\partial p}\right) + \frac{u}{a\cos\varphi}\frac{\partial}{\partial \lambda}\left(\frac{\partial \Phi}{\partial p}\right) + \frac{v}{a}\frac{\partial}{\partial \varphi}\left(\frac{\partial \Phi}{\partial p}\right) + \sigma\omega = -\frac{R}{c_p}\frac{1}{p}\frac{dQ}{dt} \quad (2.3)$$

and
$$\frac{1}{a\cos\varphi}\frac{\partial u}{\partial \lambda} + \frac{1}{a}\frac{\partial v}{\partial \varphi} - \frac{\tan\varphi}{a}v + \frac{\partial \omega}{\partial p} = 0. \quad (2.4)$$

The definition of available potential energy is written in the following form:

$$P = \frac{1}{g}\int_0^{p_0}\int_0^{2\pi}\int_{\varphi_1}^{\varphi_2}\frac{1}{2\sigma}\left(\frac{\partial \Phi}{\partial p}\right)^2 a^2\cos\varphi\, d\varphi\, d\lambda\, dp, \quad (2.5)$$

from which it follows that

$$\frac{dP}{dt} = \frac{1}{g}\int_0^{p_0}\int_0^{2\pi}\int_{\varphi_1}^{\varphi_2}\frac{1}{\sigma}\frac{\partial \Phi}{\partial p}\frac{\partial}{\partial t}\left(\frac{\partial \Phi}{\partial p}\right) a^2\cos\varphi\, d\varphi\, d\lambda\, dp. \quad (2.6)$$

In the formulas above λ is longitude, φ latitude and a is the radius of the earth.

We derive an expression for the rate of change of the zonal available potential energy by first averaging (2.3) with respect to latitude using the following notation:

$$\overline{(\quad)} = \frac{1}{2\pi}\int_0^{2\pi} (\quad)\, d\lambda. \tag{2.7}$$

We find

$$\frac{\partial}{\partial t}\left(\frac{\partial \bar{\Phi}}{\partial p}\right) + \frac{1}{a\cos\varphi}\frac{\partial\left(\overline{v\dfrac{\partial \Phi}{\partial p}\cos\varphi}\right)}{\partial \varphi} + \sigma\bar{\omega} = -\frac{R}{c_p}\frac{1}{p}\frac{d\bar{Q}}{dt}. \tag{2.8}$$

After multiplying (2.8) by

$$\frac{1}{\sigma}\frac{\partial \bar{\Phi}}{\partial p}$$

we can derive the following equation for the rate of change of $\bar{P}$

$$\frac{d\bar{P}}{dt} = -C(\bar{P},P') - C(\bar{P},\bar{K}) + G(\bar{P}), \tag{2.9}$$

where

$$C(\bar{P},P') = \frac{2\pi a}{g}\int_0^{p_0}\int_{\varphi_1}^{\varphi_2}\frac{1}{\sigma}\frac{\partial \bar{\Phi}}{\partial p}\frac{\partial\left(\overline{v\dfrac{\partial \Phi}{\partial p}\cos\varphi}\right)}{\partial \varphi}\, d\varphi\, dp, \tag{2.10}$$

$$C(\bar{P},\bar{K}) = \frac{2\pi a^2}{g}\int_0^{p_0}\int_{\varphi_1}^{\varphi_2}\bar{\omega}\frac{\partial\bar{\Phi}}{\partial p}\cos\varphi\, d\varphi\, dp, \tag{2.11}$$

$$G(\bar{P}) = -\frac{R}{c_p}\frac{2\pi a^2}{g}\int_0^{p_0}\int_{\varphi_1}^{\varphi_2}\frac{1}{\sigma p}\frac{\partial\bar{\Phi}}{\partial p}\frac{d\bar{Q}}{dt}\cos\varphi\, d\varphi\, dp. \tag{2.12}$$

(2.9) shows that the rate of change of zonal available potential energy is determined by the generation of this form of energy by diabatic processes and by transformations to zonal kinetic energy and eddy available potential energy. The magnitude of $G(\bar{P})$ has been calculated by Wiin-Nielsen and Brown (1960), while the transformation to zonal kinetic energy which depends upon the mean meridional circulation has been computed, for example, by Wiin-Nielsen (1959). It is the transformation between zonal and eddy available potential energy which we want to calculate. The integral is given in (2.10). The following sections will describe the method of calculation of $C(\bar{P},P')$.

The data available for the calculations were the routine objective height analyses from the National Meteorological Center for the levels 850, 700, 500, 300 and 200 mb. Due to the limited vertical resolution it is necessary to make a numerical integration with respect to pressure. The contribution to $C(\bar{P},P')$ from a layer of pressure difference can be written

$$C_\Delta(\bar{P},P') = \frac{2\pi g a}{\sigma \Delta p}\int_{\varphi_1}^{\varphi_2}\bar{h}\frac{\partial(\overline{hv}\cos\varphi)}{\partial\varphi}\, d\varphi, \tag{2.13}$$

where we also have approximated the derivative with respect to pressure in the following way

$$\frac{\partial \Phi}{\partial p} = -\frac{gh}{\Delta p}, \tag{2.14}$$

where h is the thickness of the layer, and where σ is a mean value for the layer.

The formula (2.13) can be used as it stands but it will be of importance to arrange the calculations in such a way that we also get information about the transport of heat. This quantity is defined by

$$TH(\varphi) = \frac{1}{g}\int_0^{p_0}\int_0^{2\pi} c_p T v a\cos\varphi\, d\lambda\, dp \tag{2.15}$$

which measures the transport of heat across the latitude φ from the top of the atmosphere to the standard pressure $p = p_0$.

The contribution to the heat transport across the latitude circle φ from the same layer of pressure difference Δp is

$$TH_\Delta(\varphi) = \frac{\Delta p\, a}{g} c_p \cos\varphi \int_0^{2\pi} \tilde{T}\tilde{v}\, d\lambda, \tag{2.16}$$

where $\tilde{T}$ and $\tilde{v}$ are vertical mean quantities for the layer. It is well known that mean temperature in a layer is related to the thickness h by the formula

$$h = \frac{R}{g}\tilde{T}\ln\left(\frac{p_1}{p_2}\right), \tag{2.17}$$

where p_1 is the pressure at the lower boundary of the layer and p_2 the pressure at the upper boundary. Using (2.17) we find that

$$TH_{\Delta}(\varphi) = \Delta p \frac{c_p}{R} a \cos\varphi \frac{1}{\ln\left(\frac{p_1}{p_2}\right)} 2\pi \overline{h\tilde{v}} \quad (2.18)$$

which is the formula from which the heat transport can be computed from the height fields.

When we integrate (2.13) by parts and neglect the boundary integrals which would vanish if our region were the whole sphere we may write (2.13) in the form

$$C_{\Delta}(\bar{P}, P') = -\frac{g}{\sigma(\Delta p)^2} \ln\left(\frac{p_1}{p_2}\right) \frac{R}{c_p} \int_{\varphi_1}^{\varphi_2} TH_{\Delta}(\varphi) \frac{\partial \bar{h}}{\partial \varphi} d\varphi. \quad (2.19)$$

Thus we see that the conversion of zonal available potential energy to eddy available potential energy depends upon the relation between the transport of heat and the meridional gradient of the zonally averaged thickness field. Since it is well known that the transport of heat is positive at almost all latitudes and that $\partial\bar{h}/\partial\varphi$ is negative, it can immediately be seen that $C(\bar{P},P')$ must turn out to be positive, which means that eddy available potential energy is being generated through conversion from zonal available potential energy.

The contributions from the layers evaluated according to (2.19) were finally added in order to get the complete integral in (2.10). In the numerical integration with respect to pressure we have applied the weight 2 to the layer between 850 and 700 mb and the weight 3 to the layer 300 to 200 mb in order to complete the integration with respect to pressure.

The next problem is to write (2.19) in the domain of wave number. In order to do this we return to (2.18) and write the thickness field h as the following Fourier series.

$$h = A_0(\varphi) + \sum_{n=1}^{\infty} (A_n(\varphi) \cos n\lambda + B_n(\varphi) \sin n\lambda). \quad (2.20)$$

Furthermore let the streamfunction corresponding to the mean wind be written

$$S = a_0(\varphi) + \sum_{n=1}^{\infty} (a_n(\varphi) \cos n\lambda + b_n(\varphi) \sin n\lambda). \quad (2.21)$$

The meridional component, $\tilde{v}$, which enters in (2.18) is related to S by the relation

$$\tilde{v} = \frac{1}{a\cos\varphi} \frac{\partial S}{\partial \lambda}. \quad (2.22)$$

Using (2.20), (2.21) and (2.22) we can write the expression for the transport of heat in the form

$$TH_{\Delta}(\varphi) = \sum_{n=1}^{\infty} TH_{\Delta,n}(\varphi), \quad (2.23)$$

where

$$TH_{\Delta,n}(\varphi) = \pi\Delta p \frac{c_p}{R} \frac{1}{\ln\left(\frac{p_1}{p_2}\right)} n \times \left\{A_n(\varphi)\, b_n(\varphi) - B_n(\varphi)\, a_n(\varphi)\right\}. \quad (2.25)$$

Substituting this expression in (2.19) we find that the conversion can be written

$$C_{\Delta}(\bar{P}, P') = \sum_{n=1}^{\infty} C_{\Delta,n}(\bar{P}, P'), \quad (2.25)$$

where $$C_{\Delta,n}(\bar{P}, P') = -\frac{g \ln\left(\frac{p_1}{p_2}\right)}{2\sigma(\Delta p)^2} \frac{R}{c_p} \times \sum_{\varphi_1}^{\varphi_2} TH_{\Delta,n}(\varphi)\, [A_0(\varphi - \Delta\varphi) - A_0(\varphi + \Delta\varphi)]. \quad (2.26)$$

It is thus seen that in order to evaluate the heat transport as a function of latitude and wave number, it is necessary to compute the Fourier coefficients, $A_n(\varphi)$ and $B_n(\varphi)$, for the thickness field in each layer and to compute the Fourier coefficients, $a_n(\varphi)$ and $b_n(\varphi)$, for the stream function, S, for the mean wind in each layer. The Fourier coefficients for a given field were computed from the data given in the grid points of the octagonal grid used by the National Meteorological Center by first interpolating the data to a latitude–longitude grid using 2½ degree grid-sizes for both latitude and longitude and next compute the Fourier coefficients for the interpolated data for each latitude. This procedure gives a horizontal resolution which is much too high in the high latitudes, but reasonable in middle and low latitudes. Only the first 15 Fourier components were computed. It was furthermore decided that the data were too sparse and the analysis too uncertain to do calculations south of 17.5° N. In the evaluation of (2.24) the lower latitude was therefore 17.5° N, which means that φ_1 in (2.26) is 20° N while φ_2 is 85° N. It should furthermore be mentioned that the streamfunction, S, is not the solution to the complete balance equation, but is the "geostrophic" streamfunction, introduced by SHUMAN (1957). S is therefore the solution to the equation

$$\nabla^2 S = \nabla \cdot \left(\frac{1}{f}\nabla\Phi\right). \tag{2.27}$$

The streamfunctions, S, and the Fourier coefficients were obtained for the observation times 00 Z and 12 Z for each of the days of the months of January 1962. The result of the calculations is therefore a record of the heat transport for all the different latitudes for the first 15 Fourier components and the energy conversion for zonal to eddy available potential energy for the same components. The result of the computations will be described in Sections 4 and 5.

3. Conversion between eddy and zonal kinetic energy

The expression for conversion between eddy and zonal kinetic energy is most easily derived from the first equation of motion which we write in the following form:

$$\frac{\partial u}{\partial t} + \frac{u}{a\cos\varphi}\frac{\partial u}{\partial\lambda} + \frac{v}{a}\frac{\partial u}{\partial\varphi} + \omega\frac{\partial u}{\partial p} = -\frac{1}{a\cos\varphi}\frac{\partial\Phi}{\partial\lambda} + fv + \frac{uv\tan\varphi}{a} + F_x. \tag{3.1}$$

F_x is the frictional force per unit mass. Note that u and v in the horizontal part of the advective acceleration are going to be considered non-divergent. Note, furthermore, that this assumption means that $\bar{v} = 0$. When we make use of the continuity equation (2.4) we obtain after averaging along the latitude circle

$$\frac{\partial\bar{u}}{\partial t} = -\frac{1}{a\cos^2\varphi}\frac{\partial(\overline{uv}\cos^2\varphi)}{\partial\varphi} - \frac{\partial\overline{u\omega}}{\partial p} + \bar{F}_x. \tag{3.2}$$

from which it follows that

$$\frac{\partial}{\partial t}\left(\frac{1}{2}\bar{u}^2\right) = -\frac{\bar{u}}{a\cos^2\varphi}\frac{\partial(\overline{uv}\cos^2\varphi)}{\partial\varphi} - \bar{u}\frac{\partial(\overline{u\omega})}{\partial p} + \bar{u}\bar{F}_x. \tag{3.3}$$

The kinetic energy of the zonal flow is by definition

$$\bar{K} = \frac{2\pi}{g}\int_0^{p_0}\int_{\varphi_1}^{\varphi_2}\frac{1}{2}\bar{u}^2 a^2\cos\varphi\, d\varphi\, dp \tag{3.4}$$

and the rate of change of the kinetic energy is

$$\frac{d\bar{K}}{dt} = \frac{2\pi}{g}\int_0^{p_0}\int_{\varphi_1}^{\varphi_2}\frac{\partial(\frac{1}{2}\bar{u}^2)}{\partial t}a^2\cos\varphi\, d\varphi\, dp. \tag{3.5}$$

We obtain therefore from (3.3)

$$C(K',\bar{K}) = -\frac{2\pi a}{g}\int_0^{p_0}\int_{\varphi_1}^{\varphi_2}\frac{\bar{u}}{\cos\varphi}\frac{\partial(\overline{uv}\cos^2\varphi)}{\partial\varphi}d\varphi\, dp \tag{3.6}$$

which also, after integration by parts and neglecting the boundary integral, can be written

$$C(K',\bar{K}) = \frac{2\pi a}{g}\int_0^{p_0}\int_{\varphi_1}^{\varphi_2} \times\left[\overline{uv}\cos^2\varphi\frac{\partial}{\partial\varphi}\left(\frac{\bar{u}}{\cos\varphi}\right)\right]d\varphi\, dp. \tag{3.7}$$

(3.6) and (3.7) measure only the energy transformation by horizontal processes. A more complete evaluation will also have a term coming from the vertical transport of momentum, but our data do not allow us to evaluate this term.

The transformation from eddy kinetic to zonal kinetic energy is therefore determined essentially by the correlation between the momentum transport and the meridional shear of the mean zonal wind. In order to express this integral in the domain of wave numbers we return to the momentum transport which we define as

$$TM(\varphi) = \overline{uv} = \overline{u'v'} \tag{3.8}$$

because in our formulation $\bar{v} = 0$.

The transport of angular momentum can be obtained from $TM(\varphi)$ by multiplying by the factor $2\pi a^2\cos^2\varphi$. Using again the Fourier

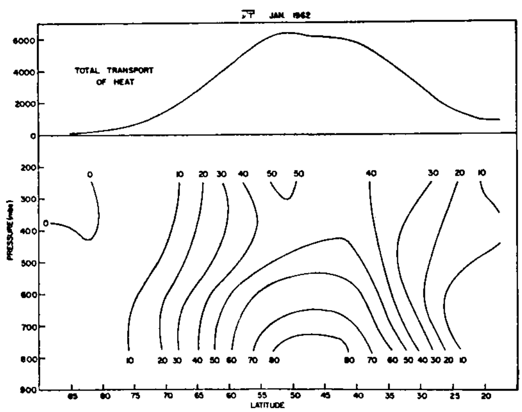

FIG. 1. The averaged transport of sensible heat for the month of January 1962 as a function of latitude and pressure in the unit 10^9 kj cb^{-1}sec^{-1} (lower part). The total transport of heat across a latitude circle as a function of latitude in the unit 10^9 kj sec^{-1} (upper part).

series (2.21) for the geostrophic stream function, S, it is easily seen that (3.8) can be written in the form

$$TM(\varphi) = \sum_{n=1}^{\infty} TM_n(\varphi), \tag{3.9}$$

where

$$TM_n(\varphi) = \frac{n}{2a^2 \cos\varphi} \left\{ a_n \frac{\partial b_n}{\partial \varphi} - b_n \frac{\partial a_n}{\partial \varphi} \right\}. \tag{3.10}$$

Using these expressions for the momentum transport we can finally write the energy conversion in the form

$$C(K', \bar{K}) = \sum_{n=1}^{\infty} C_n(K', \bar{K}) \tag{3.11}$$

with

$$C_n(K', \bar{K}) = \frac{2\pi a}{g} \int_0^{p_0} \int_{\varphi_1}^{\varphi_2} TM_n(\varphi) \cos^2\varphi \frac{\partial}{\partial \varphi} \times \left(- \frac{\partial a_0}{a \cos\varphi \partial \varphi} \right) d\varphi dp. \tag{3.12}$$

The integral (3.12) was evaluated using the geostrophic streamfunctions, S, for the levels 850, 700, 500, 300 and 200 mb. In making the numerical integrations with respect to pressure the following weights were applied: 22.5, 17.5, 20.0, 15.0 and 25.0 corresponding to the levels as stated above. The use of this procedure will probably give too large a weight to the highest levels in the atmosphere because the 200 mb levels are taken to represent the total layer from the top of the atmosphere to the 250 mb level. It will therefore be important in the future to incorporate one or more stratospheric levels in the calculations. The evaluation of the momentum transports and the transformation between the two forms of kinetic energy were otherwise made using the same general scheme as described in section 2.

The derivation in this and the previous section is simplified by the fact that we have only found it necessary to consider the zonal form of the energies. A more complete treatment of the equation can be found in SALTZMAN (1957).

4. The Heat Transport

In this section we are going to describe the results which have been obtained for the month of January 1962 regarding the transport of heat in the wave-number regime.

Fig. 1 gives the transport of heat as a function of latitude and pressure when the contribution of the first 15 Fourier components are added. The upper part of Fig. 1 gives the total transport of heat across the latitude circle integrated over the total depth of the atmosphere. The unit of the upper curve is 10^9 kj sec^{-1}. Fig. 1 shows that the heat transport is almost everywhere toward the north with the exception of a small region in the high latitudes at low pressures. The maximum heat transport occurs in the middle latitudes at low elevations. The line of maximum transport tends toward lower latitudes as we go up through the atmosphere to about 400 mb. A secondary maximum occurs in the highest layer (300–200 mb) at about 52.5° N. In the integrated heat transport we find a very broad maximum centered around 45° N.

The heat transport in Fig. 1 may be thought of as the transport of heat including all wave numbers because the transport carried out by waves with a wave number larger than 15 is negligible in our data. We can therefore compare this transport with the results of other calculations where no break-down in the wave number was attempted. One such calculation has been carried out by WHITE (1954), who has computed the flux of sensible heat for the entire year 1950. His maximum transport occurs at 850 mb and at 55° N. The maximum value is 40×10^9

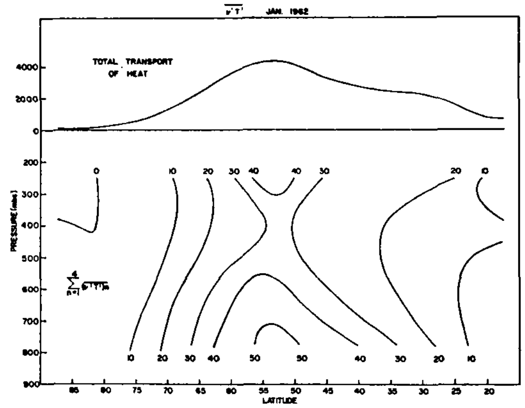

FIG. 2. The averaged transport of sensible heat for the month of January 1962 by the waves with wave number $n = 1$, 2, 3 and 4 as a function of latitude and pressure (lower part). The total transport of heat across a latitude circle as a function of latitude (upper part). Units as in Fig. 1.

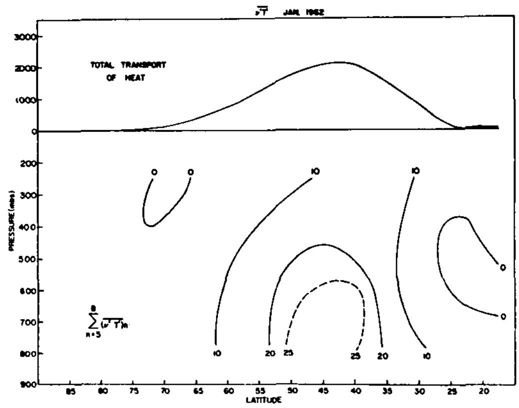

FIG. 3. As Fig. 2, but with $n = 5$, 6, 7 and 8.

$\mathrm{kj\,cb^{-1}sec^{-1}}$ or about half the value of the maximum found in the calculation for the single month, January 1962. One will naturally expect differences of this nature between the yearly average and a single month representing the time of the year where there is most likely a maximum transport of heat.

It is next our purpose to investigate the transport of heat in the wave number regime. We could do this by preparing diagrams similar to Fig. 1 for each of the 15 different wave numbers, but we have preferred to group the fifteen components into three groups, the first consisting of wave numbers 1 to 4 which represents, by and large, what we refer to as the planetary scale or the ultra long waves, next a group consisting of wave numbers 5 to 8 which at least in middle latitudes represents the baroclinically unstable waves and finally a group consisting of wave numbers 9 to 15. At 45° N the first group covers wave-lengths from about 28,000 km to 7000 km, the second group from 7000 km to 3500 km, while the third group has wave-lengths from 3500 km to about 1900 km. Fig. 2 gives the transport of heat by the first four wave numbers in a diagram exactly analogous to Fig. 1. One notices the very great similarity between the patterns in Fig. 1 and Fig. 2. The maxima occur approximately in the same position. The important fact to be noticed from Fig. 2 in comparison with Fig. 1 is that the waves corresponding to the four smallest wave numbers transport more than half of the sensible heat. It is customary to judge the performance of numerical general circulation studies by comparing the transports of heat and momentum and the energetics of the models with similar observational studies of atmospheric data. It is evident from Fig. 2 that any model of the atmosphere which is being used to study the general circulation by numerical experiment must contain a mechanism which generates and maintains the ultra-long waves if it is supposed to duplicate the developments in the real atmosphere. The studies of the general circulation by numerical experiments which have been published so far (PHILLIPS, 1956; SMAGORINSKY, 1963) does not contain ultra-long waves with any appreciable amplitude. In Phillips' experiment the ultra-long waves cannot exist simply because the longitudinal dimension is a rather small fraction of the total circumference of the earth. Smagorinsky's calculation does not produce ultra-long waves, presumably, because the model does not contain any continents (with topography) and oceans which through their kinematic and thermal influences excite waves of numbers 2 and 3. The present calculation shows that the thermal structure of the ultra-long waves is such that they are responsible for a major portion of the heat transport, which means that the temperature field is lagging behind the pressure field on each isobaric surface.

Fig. 3 shows the heat transport carried out by waves with wave numbers 5 to 8. Very small transport of sensible heat is found in the

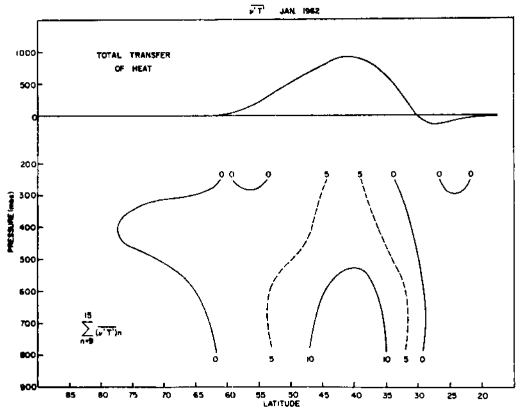

FIG. 4. As Fig. 2, but with $n = 9, 10, \ldots, 15$.

high latitudes for these wave numbers which of course correspond to very short waves in the arctic regions. As an example we might mention that wave number 5 at 70° N has a wave-length of about 2700 km. In the middle latitudes we find a maximum of a little more than 25×10^9 kj cb^{-1}sec^{-1} at about 42.5° N, or in other words about $\frac{1}{3}$ of the total transport. The distribution of the heat transport for wave numbers 5 to 8 has a fair resemblance to the total transport but is a smaller fraction than the contribution from the ultra-long waves. Fig. 4 shows the contribution from wave numbers 9 to 15 to the heat transport. The maximum is again found in middle latitudes and at low elevations, but the amounts are small compared with the total transports.

In order to get some insight into the spectra of the heat transports we have prepared Fig. 5 which shows the total transport of heat from $p = 0$ to $p = p_0$ across different latitude circles as a function of wave number. At 60° N we find a pronounced maximum at $n = 2$. The amounts for $n = 9$ to 15 for this latitude are so small that they have been excluded from the figure. The maximum for $n = 2$ is also very marked at 50° N, which is the latitude closest to the maximum heat transport. At 40° N we find that the heat transport for $n = 2$ has decreased considerably, while there is a general increase in the heat transport for higher wave numbers. The heat transports at low latitudes are small and somewhat erratic.

The heat transport spectra for each of the layers 850–700, 700–500, 500–300 and 300–200 mb are reproduced in Fig. 6 for the latitudes 60, 50, 40, 30 and 20° N. The maximum for $n = 2$ is apparent in all the layers at 60 and 50° N. It is furthermore evident from Fig. 6 that the heat transports in the different layers are closely related.

5. The momentum transport

It is the purpose of this section to describe the results of the momentum transport calculations for the month of January 1962 in the domain of wave number.

The lower part, Fig. 7, shows the momentum transport as a function of latitude and pressure, while the upper part of the figure shows a

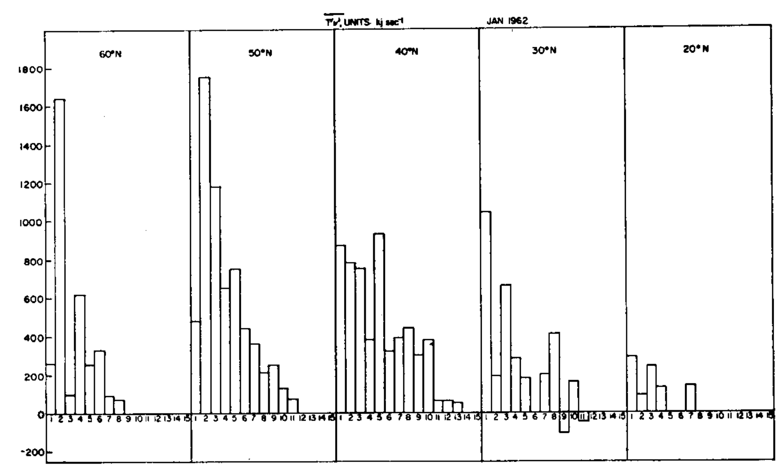

FIG. 5. The total transport of heat across a latitude circle as a function of wave number for selected latitudes. Averaged values for the month of January 1962.

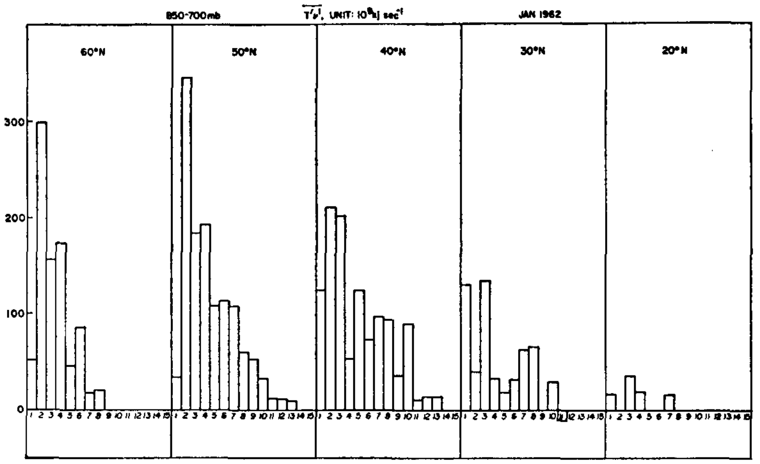

Fig. 6*a*. The transport of heat across a latitude circle in the layer 850–700 mb as a function of wave number for selected latitudes. Averaged values for the month of January 1962.

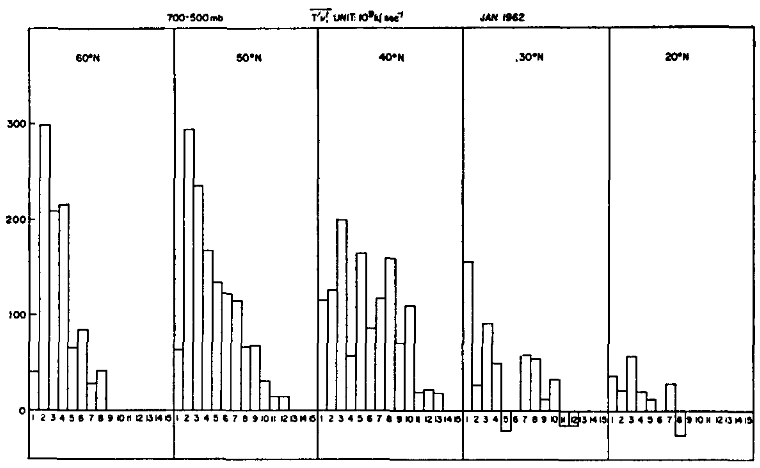

Fig. 6*b*. As Fig. 6*a*, but for the layer 700–500 mb.

weighted average of the momentum transport over all the five levels as a function of latitude. The unit in both parts of the figure is $m^2 sec^{-2}$. We notice that the momentum transport south of 56° N is towards the north, while we find a southward transport north of this latitude. The maximum northward transport is found at 200 mb and at about 35° N, while the maximum transport toward the south is found at 300 mb and at 65° N. In the following we shall discuss how great a fraction of the momentum transport is carried out by the waves of wave numbers 1 to 4, wave numbers 5 to 8 and wave numbers 9 to 15 just as we did for the heat transport.

The momentum transport by waves of wave numbers 1 to 4 is shown in Fig. 8. A comparison of Fig. 7 and Fig. 8 shows that the distribution of the momentum transport in the meridional cross-section is very similar. In the region of southward transport in the high latitudes we find again a maximum at 65° N and at 300 mb. Almost the entire momentum transport is found in the first four wave numbers. The maximum northward momentum transport in the first four wave numbers is found at 32.5° N and 200 mb. It amounts to about 50 % of the total momentum transport. We find, therefore, a situation in the results of the momentum

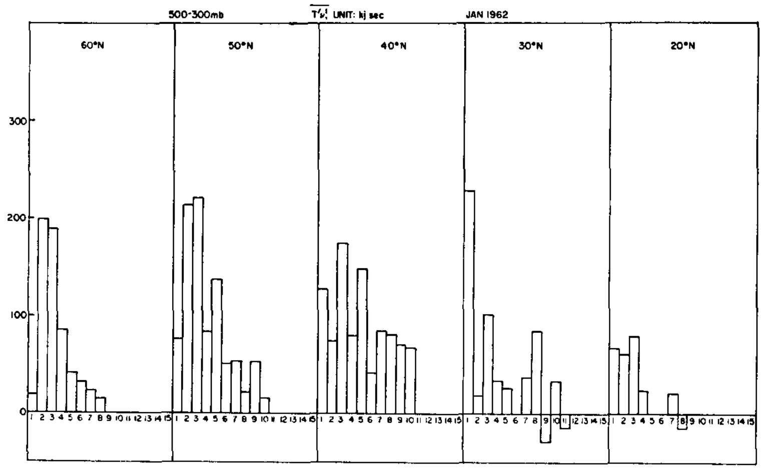

FIG. 6c. As Fig. 6a, but for the layer 500–300 mb.

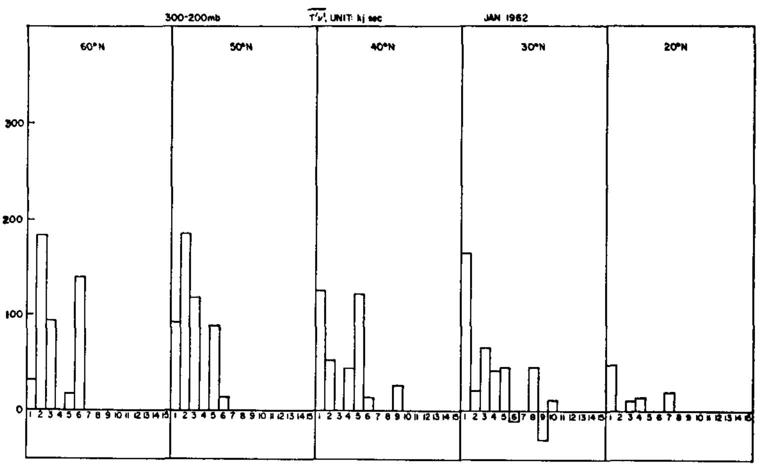

FIG. 6d. As Fig. 6a, but for the layer 300–200 mb.

transport calculation which is very similar to the situation which resulted from the heat transport calculation to the extent that the waves of wave numbers 1 to 4 account for almost all the transport in the high latitudes while about 50 % of the transport in the low latitudes is carried out by the longest waves.

The transport of momentum by the next four waves (5 to 9) in the wave number domain can be seen in Fig. 9 which shows that only about 20 % of the total southward transport is carried out by these waves, while about 30 % of the northward transport is accounted for by waves of wave numbers 5 to 9. One notices further that the zero line in the diagram has now shifted somewhat towards the south. This zero line has shifted further to the south in Fig. 10 which shows the momentum transport of the waves with wave numbers 9 to 15. While the southward transport of momentum in the high latitudes is almost negligible for these waves, we find that the northward transport around 30–35° N is still about 10 % of the total transport.

The main conclusions from the study of the momentum transport in the wave-number regime are therefore very much the same as they were from the study of the transport of sensible heat. The ultra-long waves account for a very large fraction of the total transport of

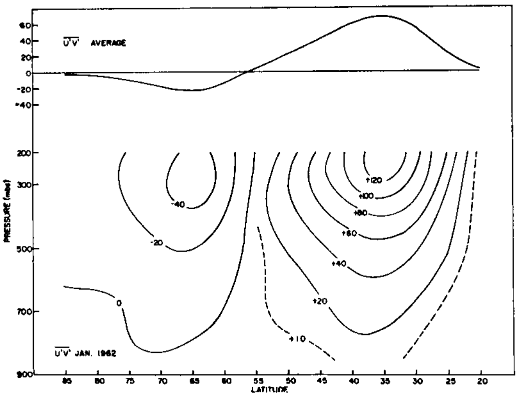

FIG. 7. The transport of momentum in the unit $m^2 sec^{-2}$ as a function of latitude and pressure (lower part). The momentum transport averaged with respect to pressure as a function of latitude (upper part). Averaged data for January 1962.

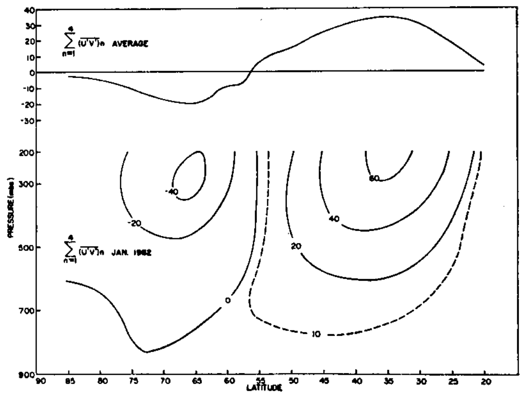

FIG. 8. The transport of momentum by waves with wave number $n = 1$, 2, 3 and 4. Arrangement and units as in Fig. 7.

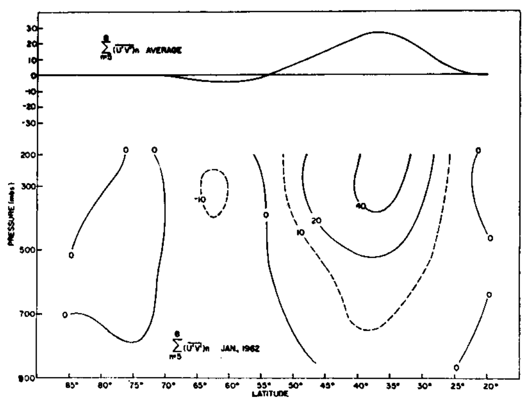

FIG. 9. As Fig. 8, but with $n = 5$, 6, 7 and 8.

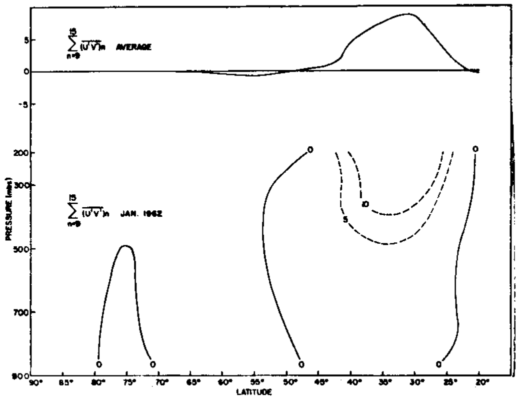

FIG. 10. As Fig. 8, but with $n = 9, 10, \ldots, 15$.

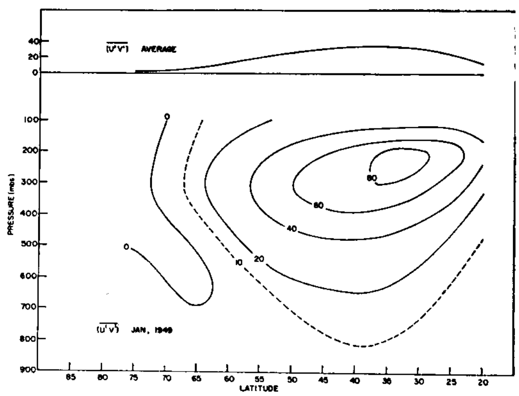

FIG. 11. The transport of momentum in the unit $m^2 sec^{-2}$ for the month of January 1949 according to Mintz. Arrangement as in Fig. 7.

momentum and must be an integral part of any study of the general circulation by numerical experiment. A conclusion similar to the one mentioned above was also reached by ELIASEN (1958) who compared the momentum transports of the waves with wave numbers 1 to 3 on the normal maps for January with the total geostrophic poleward transport of momentum as calculated by MINTZ (1951). In order to investigate the differences in the momentum transport between different winter months we can compare the geostrophic transport computed by MINTZ (loc. cit.) for the month of January 1949 with our transports for January 1962. Fig. 11 was prepared from Mintz' data converted to the unit $m^2 sec^{-2}$. While Mintz did not have 850 mb data, his investigation covers a greater depth of the atmosphere because he had 100 mb data. The

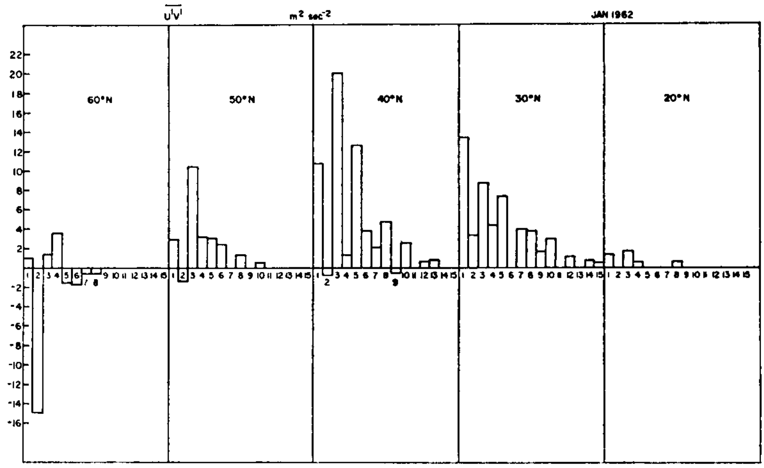

FIG. 12. Momentum transport averaged with respect to pressure as a function of the wave number for selected latitudes. Averaged values for the month of January 1962.

highest latitude considered by him is 75° N. The comparison between Fig. 11 and Fig. 7 shows that the maximum momentum transport in the low latitudes occurs at almost the same place, but that the transport in January 1949 is only about $\frac{2}{3}$ of the transport in January 1962. It will furthermore be noticed that the transports in January 1949 are positive almost everywhere. The line of zero transport is located around 65–70° N in this month, while the zero-line in January 1962 is about 10° further south. Although the pattern in Fig. 7 and Fig. 11 is similar in many respects, it is evident that a single month cannot be considered representative.

Fig. 12 shows the spectra of the momentum transport for five selected latitudes: 60, 50, 40, 30 and 20° N. The spectra represents a weighted average of the computations at the five information levels. It is worthwhile noticing that the wave, $n = 2$, is responsible for a very large fraction of the total momentum transport at 60° N, while the wave, $n = 3$, is dominating at 50° N and 40° N together with wave numbers 1 and 5. The spectra in Fig. 12 can be compared with those computed by SALTZMAN (1958), who used data from the month of January 1949. There is indeed a great similarity between some of the spectra presented by SALTZMAN (loc. cit.) and those represented in Fig. 12 to the extent that both calculations show the importance of disturbances of wave numbers 3 and 5 in carrying out the total momentum transport. It is evident from Fig. 12 that it will be necessary to have a longer time series of momentum transports in order to get significant spectra.

6. Changes in the zonal mean caused by horizontal processes

The equations (2.8) and (3.2) express the rate of change of $\partial\bar{\Phi}/\partial p$ and $\bar{u}$. It is seen from the former equation that the vertical derivative of the mean geopotential is changed due to three processes: the horizontal convergence of the heat transport, the mean meridional circulation and the diabatic processes. From the material presented in this paper it is possible to evaluate the effect of the first process which can be conveniently expressed as the rate of change in the zonal mean of the temperature. When the hydrostatic relation is used to introduce the temperature in (2.8) we can transform the equation into the following form:

$$\frac{\partial \bar{T}}{\partial t} = -\frac{1}{a\cos\varphi}\frac{\partial(\overline{vT}\cos\varphi)}{\partial\varphi} + \frac{p\sigma}{R}\bar{\omega} + \frac{1}{c_p}\frac{\overline{dQ}}{dt}. \quad (6.1)$$

The heat transport per unit isobaric layer is according to (2.16)

$$TH^*(\varphi) = \frac{a}{g}c_p 2\pi\cos\varphi\,\overline{vT} \quad (6.2)$$

which means that (6.1) can also be written in the following form:

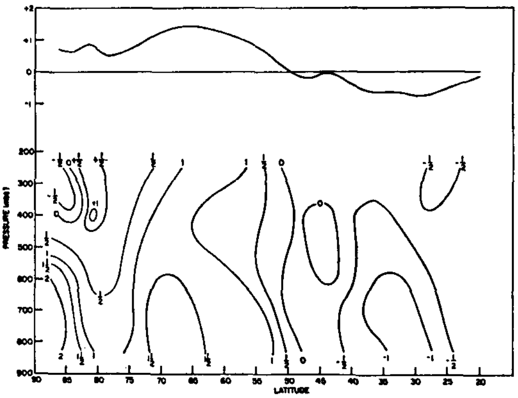

FIG. 13. The change in the zonal mean of the temperature due to meridional convergence of the heat transport as a function of latitude and pressure (lower part). The change in the vertical average of the zonal mean of the temperature due to meridional convergence of the heat transport as a function of latitude (upper part). Averaged values for the month of January 1962. Unit: deg day^{-1}.

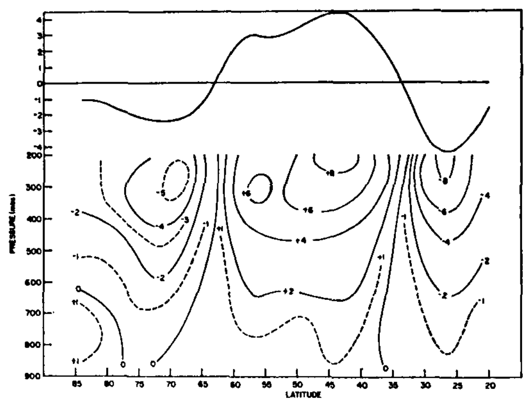

FIG. 14. The change in the zonal mean of the zonal wind component due to meridional convergence of the momentum transport as a function of latitude and pressure (lower part). The change in the vertical average of the zonal mean wind component due to meridional convergence of the momentum transport as a function of latitude (upper part). Averaged values for the month of January 1962. Unit: m sec^{-1}day^{-1}.

$$\frac{\partial \overline{T}}{\partial t} = -\frac{g}{2\pi c_p a^2 \cos\varphi}\frac{\partial TH^*}{\partial \varphi} + \frac{p\sigma}{R}\overline{\omega} + \frac{1}{c_p}\frac{\overline{dQ}}{dt}. \quad (6.3)$$

The first term in (6.3) has been evaluated from the average monthly data of the heat transport as shown in Fig. 1. We have found it convenient to express the result in the unit deg day^{-1}. The result is shown in Fig. 13 where the temperature change is plotted as a function of latitude and pressure in the lower part of the figure, while the upper part shows the weighted vertical average. It is first of all seen from Fig. 13 that the main effect of the horizontal processes on the zonal mean of the temperature field is to produce an increase in the temperature in the northern half of the hemisphere, while a decrease in $\overline{T}$ is found in the low latitudes. The increase in $\overline{T}$ is largest at low elevations in the very high latitudes (2 deg day^{-1}). We find a second maximum in the latitude belt 60–70° N where the increase in $\overline{T}$ in the lower part of the troposphere amounts to 1.5 deg day^{-1} decreasing to a little more than 1 deg day^{-1} in the 200–300 mb layer. South of about 50° N there is, in general, a decrease in $\overline{T}$. The largest decrease is found at low elevations at 30° N (-1 deg day^{-1}) with decreasing values as we go up through the atmosphere.

We are next going to evaluate the change in the mean zonal flow due to horizontal non-divergent processes. This can be done from the average monthly data for the momentum transport by computing the first term on the right-hand side of (3.2). We have expressed the result of this calculation in the unit of m sec^{-1}day^{-1}, and the result of the calculation is shown in Fig. 14. where the change in the mean zonal wind due to horizontal convergence of momentum is drawn as a function of pressure and latitude in the lower part of the figure. The upper part of Fig. 14 shows the weighted vertical average of the change in the zonal component of the wind due to horizontal non-divergent processes. Another interpretation of the upper curve is that it shows the rate of change in the vertically integrated zonal component of the wind. This means that the upper curve also shows the type of changes which one on the average will expect to find in a non-divergent, equivalent barotropic model, which therefore on the average will predict an increase of the zonal component in the middle latitudes (35–65° N) and a decrease to the north and the south of this latitude region. It is interesting in this respect to note that the *errors* in the zonal average of the wind found in operational forecasting with a non-divergent, barotropic model applied to 500 mb (BRISTOR, 1959) have a distribution with respect to latitude which is very similar to the upper curve in Fig. 14.

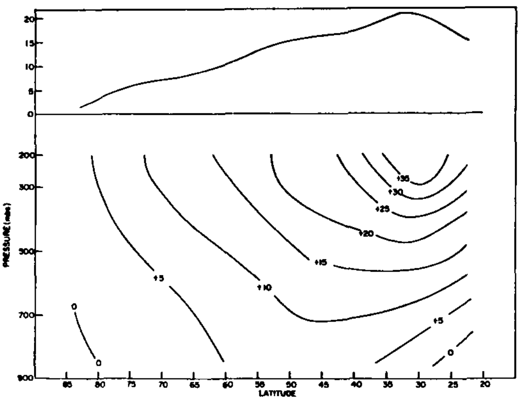

Fig. 15. Meridional cross-section of the mean zonal wind component for January 1962. Unit $m\,sec^{-1}$.

Naturally, the implication is that other effects such as the vertical transport of momentum, the mean meridional circulation and frictional effects must counteract the meridional convergence of momentum. It is beyond the scope of this paper to investigate these processes in detail.

The lower part of Fig. 14 shows that the convergence of momentum causes an increase in the averaged zonal component of the wind in middle latitudes at all the levels investigated in this study. Except for the levels 850 mb and 700 mb where we also find an increase in the very high latitudes, there is a decrease in $\bar{u}$ in the high and low latitudes. The changes in $\bar{u}$ increase with elevation and become as large as 8 $m\,sec^{-1}day^{-1}$ at 200 mb. Since such changes in the mean monthly zonal circulation are rarely observed we must conclude that the other processes which are able to change $\bar{u}$ must be even more important at these levels. The main processes in the upper troposphere are probably the convergence of the vertical transport of momentum and to a smaller extent the mean meridional circulation.

It is interesting to consider the role of meridional convergence of momentum in maintaining the mean zonal winds in the atmosphere. This question has been considered earlier by Mintz (1951). In order to investigate the same question for the month of January 1962 we have prepared Fig. 15 which shows the mean zonal component for January 1962 computed from the data at 850, 700, 500, 300 and 200 mb. It is seen that we find westerlies in the whole cross-section which covers the latitude zone from 22.5° N to 82.5° N with the exception of the very low and very high latitudes at 850 mb. A single maximum of almost 40 $m\,sec^{-1}$ is found at 200 mb at 32.5° N. The maximum zonal wind for each isobaric level is found further to the north as we go to lower elevations. The upper part of Fig. 15 shows the profile of the mean zonal wind when we have formed a vertical average.

A comparison between Figs. 14 and 15 shows that the effect of the horizontal convergence of momentum is to tend to move the jet stream maximum to the north at almost all levels. It is seen, in particular, that the maximum decrease of the mean zonal wind caused by horizontal processes is found at the southern edge of the wind maximum between 25° N and 30° N. Therefore, one cannot say that the zonal winds are maintained by the horizontal convergence of momentum.

7. Conversion of zonal to eddy available potential energy

The formulas developed in Section 2 of this paper were used to compute the conversion between zonal available potential energy and eddy available potential energy, $C(\bar{P},P')$ in the domain of wave number. The basic formula is (2.26) from which we can compute the conversion between the zonal available potential energy and the eddy available potential energy contained in the wave of wave number n. The information necessary to perform the integration is the meridional transport of heat and the meridional gradient of the mean zonal temperature. It was assumed in the calculations that the measure of static stability, σ, is constant in each isobaric surface, but varies with pressure. This assumption is consistent with the quasi-geostrophic theory. The variation with respect to pressure was evaluated from the data given by Gates (1961). The evaluation of the integral in (2.26) was done separately for each of the layers 850–700, 700–500, 500–300 and 300–200 mb. In addition the contribution from the different layers the lower layer was weighted by a factor 2 to account for the contribution from the layer 1000–850 mb, while the uppermost layer was weighted three times to take into account the part of the atmosphere above 200 mb.

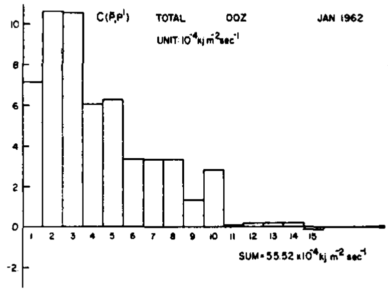

Fig. 16. The energy conversion between zonal and eddy available potential energy as a function of the wave number. Averaged data for January 1962. Unit: 10^{-4} kj m^{-2} sec^{-1}.

The result of the integration over the complete depth of the atmosphere is given in Fig. 16 where $C(\bar{P},P')$ is shown as a function of the wave number. The energy conversion $C(\bar{P},P')$ was computed for 00 Z data only. The main feature of the spectrum shown in Fig. 16 is that the conversion for all wave numbers up to $n = 14$ goes from the mean flow to the eddies. The spectrum is such that there is a well-defined maximum for $n = 2$ to 3, and with very small amounts for $n > 10$. The spectrum for $C(\bar{P},P')$ may be compared with the spectrum for the generation of eddy available potential energy, $G(P')$, computed by Wiin-Nielsen and Brown (1960) in the wave-number regime. The latter spectrum is such that eddy available potential energy is destroyed for waves of wave number less than 10 (i.e. $G(P') < 0$). The maximum destruction of P' for the month of January 1959 was found for $n = 3$. If the two months are at least qualitatively similar, we may conclude that a large fraction of the eddy available potential energy which is being generated by conversion from zonal available potential energy for the small wave numbers is being destroyed by diabatic processes due to a negative correlation between the temperature field and the heat sources. From some preliminary calculations of $G(P')$ for other months we know now that there is considerable variation in $G(P')$ through the seasons and also from one January to the next. It is therefore not possible to make any quantitative comparison between the results for two different months, but when we have obtained the results of all energy conversions based on exactly the same data, we will be able to investigate the energy budget for each wave number in the spectrum.

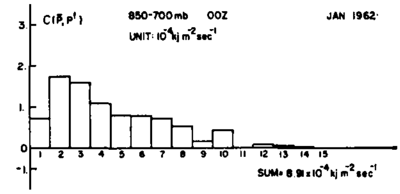

Fig. 17a. The contribution to $C(\bar{P},P')$ from the layer 850–700 mb. Arrangement as in Fig. 16.

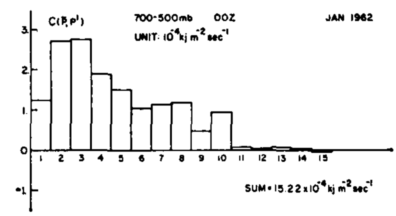

Fig. 17b. The contribution to $C(\bar{P},P')$ from the layer 700–500 mb. Arrangement as in Fig. 16.

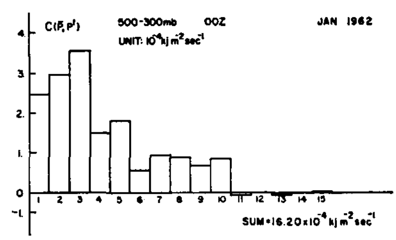

Fig. 17c. The contribution to $C(\bar{P},P')$ from the layer 500–300 mb. Arrangement as in Fig. 16.

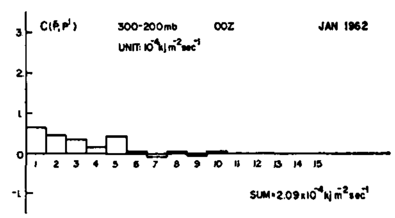

Fig. 17d. The contribution to $C(\bar{P},P')$ from the layer 300–200 mb. Arrangement as in Fig. 16.

From such investigations it will be possible to obtain certain preliminary answers to questions concerned with the non-linear transfers of energy within the spectrum between the energy on different scales. At the moment we can only notice that the eddy available potential energy is being generated from zonal available potential energy on the ultra-large scale, while the energy conversion between eddy available potential energy and eddy kinetic energy, $C(\bar{P},K')$, according to our present knowledge

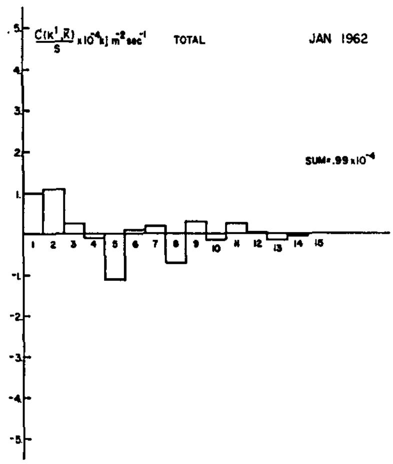

FIG. 18. The energy conversion between eddy and zonal kinetic energy as a function of the wave number. Averaged data for January 1962. Unit: 10^{-4} kj m^{-2}sec^{-1}.

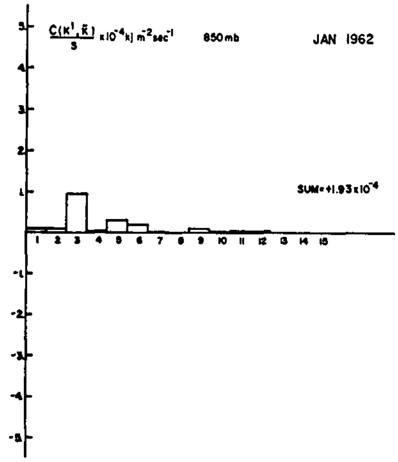

FIG. 19a. The contribution to $C(K',\bar{K})$ from the 850 mb level. Units as in Fig. 18.

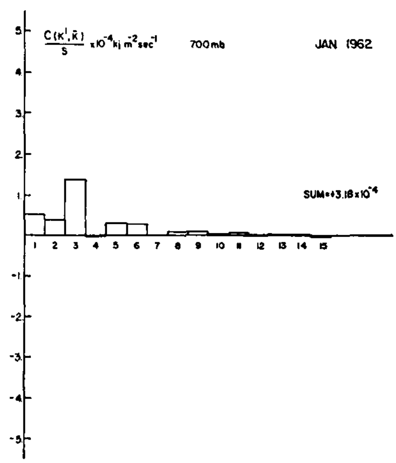

FIG. 19b. The contribution to $C(K',\bar{K})$ from the 700 mb level. Units as in Fig. 18.

(WIIN-NIELSEN, 1959) has a maximum on a smaller scale.

Fig. 17 shows the contributions from the four different layers to the total conversion $C(\bar{P},P')$ as a function of wave number. All the spectra show a maximum for $n = 1$, 2 or 3. The contributions for the different values of the wave number are in almost all cases positive. The few negative contributions are very small and appear mostly for large values of the wave number. The large contributions to $C(\bar{P},P')$ are found in the middle troposphere and to some extent in the lower troposphere, which were to be expected because of the maximum heat transport in these layers. In view of the similarity between the spectra for the different layers one can get a good first approximation to $C(\bar{P},P')$ by considering fewer information levels in each vertical column. We shall make use of this approximation in computing $C(\bar{P},P')$ for other months where the available data only covers two levels, 850 and 500 mb.

8. Conversion of eddy kinetic to mean kinetic energy

The calculations of the energy conversions from eddy kinetic to zonal energy were made from (3.12) which measures the conversion for the wave of wave number n.

The result of the calculation for the month of January 1962 when all levels were included, is shown in Fig. 18. The spectrum for $C(K',\bar{K})$ is much more irregular than the spectrum for $C(\bar{P},P')$ which was discussed in Section 7. The contribution from the waves with $n = 1,2$ and 3 is positive, while we find the largest negative contributions from the waves with $n = 5$ and $n = 8$. However, when we integrate over all wave numbers, we find that the positive contributions dominate, giving a total conversion $C(K',\bar{K})$, for the first 15 waves of 1×10^{-4}kj m^{-2}sec^{-1}.

In view of the irregularities found in the spectrum it is of interest to consider the contribution to the integral (3.12) from the different

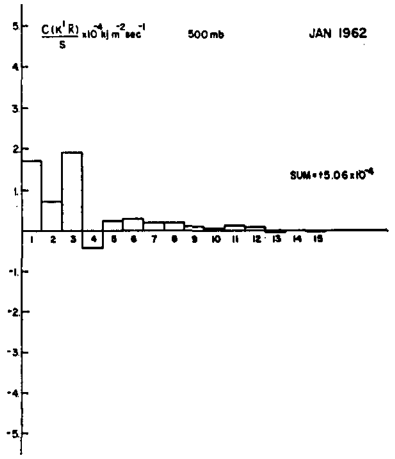

FIG. 19*c*. The contribution to $C(K',\bar{K})$ from the 500 mb level. Units as in Fig. 18.

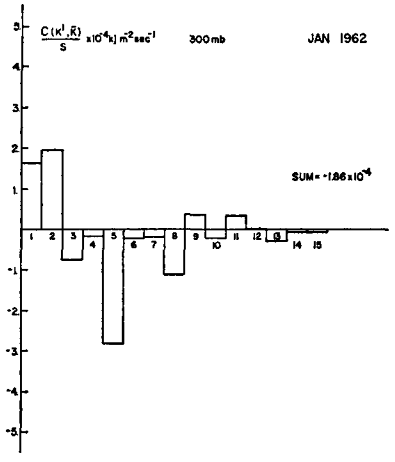

FIG. 19*d*. The contribution to $C(K',\bar{K})$ from the 300 mb level. Units as in Fig. 18.

information levels. These are reproduced in Fig. 19 which shows the contribution from the levels 850, 700, 500, 300 and 200 mb, respectively. The value marked "sum" on each of the figures is the value of $C(K',\bar{K})$ which one would get evaluating $C(K',\bar{K})$ from information at this level alone. The same statement applies for the spectra. At the two lowest levels, 850 and 700 mb, we find positive contributions for all wave numbers with a pronounced maximum for $n=3$ and a tendency for a secondary maximum for $n=5$. The contribution from the 500 mb level shows again larger positive values for the small wave numbers with a maximum for

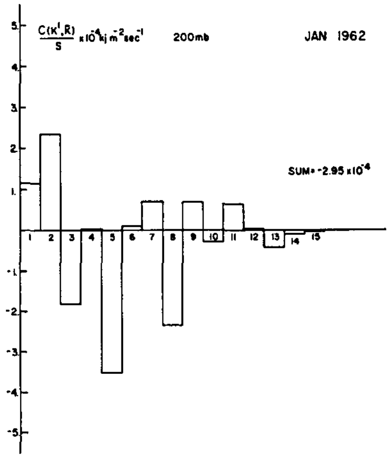

FIG. 19*e*. The contribution to $C(K',\bar{K})$ from the 200 mb level. Units as in Fig. 18.

$n=3$. The contribution for $n=4$ is negative, and we find smaller, but positive contributions for $5 \leqslant n \leqslant 12$. Due to the large positive contributions from the small wave numbers at 500 mb, the contribution from this level is larger than the contribution from the 700 mb level which again is larger than the contribution from the 850 mb level.

When we go to the 300 and 200 mb levels we find a marked change in the spectra. The waves with $n=1$ and 2 still give a positive contribution, but at 300 mb we find negative contributions for $3 \leqslant n \leqslant 8$. The situation is by and large the same at 200 mb, although the spectrum there is more irregular. When we add the contributions for the first 15 components we find negative contributions at 300 and 200 mbs.

The spectrum at 500 mb may be compared with the results obtained by SALTZMAN and FLEISHER (1960*a*). Their data cover the whole year of 1951. Our results should be compared with the winter data. The spectra for the winter of 1951 and the single month of January 1962 agree to the extent that the maximum in both cases occurs for $n=3$, that the wave with wave number 4 is a minimum and that a secondary maximum is found for $n=6$. If we had restricted our calculation to the 500 mb level we would have obtained a value of $C(K',\bar{K})$ of 5.1×10^{-4} $\mathrm{kj\,m^{-2}sec^{-1}}$. SALTZMAN and FLEISHER (loc. cit.) report a value of 5.8×10^{20} $\mathrm{ergs\,sec^{-1}}$ for the northern hemisphere which corresponds to $2.3 \times 10^{-4}\mathrm{kj\,m^{-2}sec^{-1}}$ or about half the value found in the present study. For the single month of January 1949 SALTZMAN (1958) found a value of $C(K', \bar{K})$ equal to 6.86×10^{20} ergs sec^{-1} for the latitude belt 20° N to 75° N. This value corresponds to 4.4×10^{-4} kj m^{-2} sec^{-1} which is closer to our value for January 1962 as one indeed would expect. The main result from our study is, however, that a value of $C(K', \bar{K})$ computed from the 500 mb level alone gives an overestimate of $C(K', \bar{K})$ if the month considered by us can be considered at all representative.

We may finally compare our results with those obtained by STARR (1953). He evaluated $C(K' \bar{K})$ in a number of different ways using sometimes vertically integrated values of $\bar{u}$ and sometimes time averages to evaluate the integrand in $C(K', \bar{K})$. However, the calculation performed in a way very similar to the one employed in this study using daily values, which are afterwards averaged with respect to time, gives a value of $C(K', \bar{K}) = 3.9 \times 10^{-4}$ kj m^{-2} sec^{-1} and is therefore approximately four times as large as our result. The value reported above is the largest of all the different calculations made by him. In concluding this section we may state that there is a general agreement between a number of independent calculations from different sets of data and that the energy conversion $C(K', \bar{K})$ in the winter season varies between the limits 1×10^{-4} kj m^{-2} sec^{-1} and about 4×10^{-4} kj m^{-2} sec^{-1}.

9. Concluding remarks

The most important result of the present observational study is probably that a major portion of the meridional transport of heat and momentum and of the energy conversion between the zonal mean and the eddies for both available potential energy and kinetic energy is accounted for by the waves of the lowest wave number. This conclusion emphasizes the role of the ultra-long waves in atmospheric processes and stresses the importance of the understanding of the dynamics of the planetary waves, which are poorly understood at the present time.

The present study has used the quasi-geostrophic or balanced approximation for the horizontal wind to evaluate the transports and energy conversions. It will be interesting and important to repeat the calculations using observed winds. It is apparent from the formulas employed in the present study that the calculations can be made from a knowledge of the temperature and wind fields.

A second important conclusion is that the mean conversion between zonal and eddy available potential energy is much larger than the mean conversion between eddy and zonal kinetic energy. The ratio between the two quantities as computed in this study is as large as 55. The relatively small mean energy conversion from eddy to zonal kinetic energy indicates that the zonal flow in the atmosphere has a very large amount of kinetic energy, but a relatively small exchange of energy with the reservoir of eddy kinetic energy and zonal potential energy, and consequently a small amount of frictional dissipation also.

The conversions between available potential energy and kinetic energy in the zonal flow and the eddies are unfortunately not available for January 1962. A comparison with the results obtained in this study would require a knowledge of the vertical velocity in each of the layers which have been used, that is four vertical velocities in each vertical column. However, most of the atmospheric energy conversions have been computed for the month of January 1959 except the conversions studied in this paper. A rather complete study of the energetics of the atmosphere can therefore be made if we repeat the calculations reported here for January 1959. The results of such calculations which, unfortunately, must be restricted to a two-parameter model will be described in a paper to appear in the near future.

REFERENCES

BRISTOR, C. L., 1959, Zonal wind errors in the barotropic model. *Mo. Wea. Rev.*, vol. **87**, pp. 57–63.

ELIASEN, E., 1958, A study of the long atmospheric waves on the basis of zonal harmonic analysis. *Tellus*, vol. **10**, pp. 206–216.

GATES, W. L., 1961, Static stability measures in the atmosphere. *J. Meteor.*, vol. **18**, pp. 526–533.

MINTZ, Y., 1951, The geostrophic poleward flux of angular momentum in the month of January 1949. *Tellus*, vol. **3**, pp. 195–200.

PHILLIPS, N. A., 1956, The general circulation of the atmosphere: a numerical experiment. *Quart. J. Roy. Meteor. Soc.*, vol. **82**, pp. 123–165.

SALTZMAN, B., 1957, Equations governing the energetics of the larger scales of atmospheric turbulence in the domain of wave numbers. *J. Meteor.*, vol. **14**, pp. 513–523.

SALTZMAN, B., 1958, Some hemispheric spectral statistics. *J. Meteor.*, vol. **15**, pp. 259–263.

SALTZMAN, B., FLEISHER, A., 1960*a*, Spectrum of kinetic energy transfer due to large-scale horizontal Reynolds stresses. *Tellus*, vol. **12**, pp. 110–111.

SALTZMAN, B., FLEISHER, A., 1960*b*, The modes of release of available potential energy in the atmosphere. *J. Geophys. Res.*, vol. **65**, pp. 1215–1222.

SALTZMAN, B., FLEISHER, A., 1961, Further statistics of the modes of release of available potential energy. *J. Geophys. Res.*, vol. **66**, pp. 2271–2273.

SHUMAN, F. G., 1957, Predictive consequences of certain physical inconsistencies in the geostrophic barotropic model. *Mo. Wea. Rev.*, vol. **85**, pp. 229–234.

SMAGORINSKY, J., 1963, General circulation experiments with the primitive equations, I—the basic experiment. *Mo. Wea. Rev.*, vol. **91**, pp. 99–165.

STARR, V. P., 1953, Note concerning the nature of the large-scale eddies in the atmosphere. *Tellus*, vol. **5**, pp. 494–498.

WHITE, R. M., 1954, The counter gradient flux of sensible heat in the lower stratosphere. *Tellus*, vol. **6**, pp. 177–179.

WIIN-NIELSEN, A., 1959, A study of energy conversion and meridional circulation of the large-scale motion in the atmosphere. *Mo. Wea. Rev.*, vol. **87**, pp. 319–331.

WIIN-NIELSEN, A., BROWN, J. A., 1960, On diagnostic computations of atmospheric heat sources and sinks and the generation of available potential energy. *Proc. Intern. Symp. on Numerical Weather Prediction, Tokyo*, pp. 593–613.

WIIN-NIELSEN, A., 1962, On transformation of kinetic energy between the vertical shear flow and the vertical mean flow in the atmosphere. *Mo. Wea. Rev.*, vol. **90**, pp. 311–323.